THE JOURNAL OF PHYSICAL CHEMISTRY C

Article

pubs.acs.org/JPCC

Conductance of Well-Defined Porphyrin Self-Assembled Molecular Wires up to 14 nm in Length

Quirina Ferreira,*[,†] Ana M. Bragança,[†] Luís Alcácer,[†] and Jorge Morgado[†,‡]

[†]Instituto de Telecomunicações, Instituto Superior Técnico, Av. Rovisco Pais, Lisbon, Portugal

[‡]Bioengineering Department, Instituto Superior Técnico, Universidade de Lisboa, Av. Rovisco Pais, Lisbon, Portugal

Supporting Information

ABSTRACT: We show that molecular wires up to 14 nm in length composed by zinc-porphyrins bridged by bipyridines stand efficient electrical transport. Self-assembled molecular wires were prepared step-by-step, alternating up to 13 units of zinc-octaethylporphyrin with axially coordinated 4,4′-bipyridine, on highly oriented pyrolytic graphite (HOPG). A combination of molecular resolution imaging and scanning tunneling spectroscopy allowed us to follow molecules self-assembly in real time during wire fabrication and to measure wires current, respectively. A statistical analysis of hundreds of current−voltage curves was carried out to determine the conductance of individual porphyrin/bipyridine wires. From the conductance dependence on the wires length an ultra low attenuation factor (β = 0.015 ± 0.006 Å^{-1}) was obtained for shorter wires, with a transition in conduction regime occurring at ca. 6.5 nm long wires.

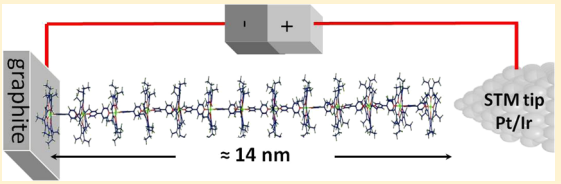

1. INTRODUCTION

Unimolecular electronics is a steady growing research area, made possible since the invention of scanning tunneling microscope (STM) and atomic force microscope (AFM). Progress is being made in terms of the understanding of conduction mechanisms and its dependence on the molecular structure, which could allow a fine-tunning of the electrical properties and, eventually, lead to true unimolecular devices (such as transistors). Yet, fundamental questions remain in view of the fact that, as mentioned below, not all results are consistent between themselves and that new molecular systems are being prepared and characterized, which are contributing to deepen our understanding on the molecular structure−electrical properties relationship.[1]

Two conductance regimes have been identified when assessing the electrical conductance of molecular wires: a tunneling regime, which dominates for shorter wires, and hopping regime, for longer conjugated wires.

The efficiency of charge transport in the tunneling regime along a wire is usually described in terms of its dependence on the length, according to eq 1:[2]

$$R = R_0 \exp(\beta d) \quad (1)$$

where R is the junction resistance, R_0 is the effective contact resistance, β is the tunneling attenuation factor, and d is the molecular wire length. In spite of the fact that eq 1 strictly applies to the charge transfer across short molecular wires, that is, in the tunnelling regime, it has also been used to characterize the transport over longer wires, where hopping transport becomes dominant.[3] A transition between these two regimes has been reported to occur in conjugated molecular wires at lengths of 4−5 nm (with β having a value of 0.09 Å^{-1} in the hopping regime).[4] Porphyrin-based molecular wires have very interesting electrical properties because they are able to transport charge efficiently over long distances.[5−7] Among the most efficient stand out the edge-fused porphyrin oligomers with lengths of up to 75 Å that transport charge efficiently across break-junctions,[8] the butadiyne-linked oligoporphyrins with low attenuation factor[9] β = 0.04 ± 0.006 Å^{-1}, and the fused tapes where the porphyrins are directly connected through three bonds, leading to a ladder-type system, locking the whole π-system in a planar conformation[6] (for which an attenuation factor β = 0.019 ± 0.0001 Å^{-1} has been determined). These are among the systems with the lowest attenuation factors.

The conductance measured in molecular wires depends not only on the intrinsic molecular properties but also on the nature of the electrodes, the type of interaction between the electrodes and the molecules (chemisorption/physisorption) and on the environment (vacuum, liquid interface, air, temperature).[10−14] A variety of methods has been used to determine the conductance of single molecules; however, all have drawbacks or limitations, and the obtained results are often not consistent.[15] This method-dependency impacts on the enormous challenges we face in understanding molecular electronics and the relationship between electrical behavior and molecular structure. Current sensing AFM (CSAFM)[16] and STM break junctions[17] are among the most used techniques to assess the electrical properties at the molecular level. In both cases, there is no gap between the molecules and the probe. CSAFM measurements are easier to perform, but the result is influenced by the tip size because usually the tip radius is

Received: January 31, 2014
Revised: March 10, 2014
Published: March 10, 2014

   dx.doi.org/10.1021/jp501122n | J. Phys. Chem. C 2014, 118, 7229−7234

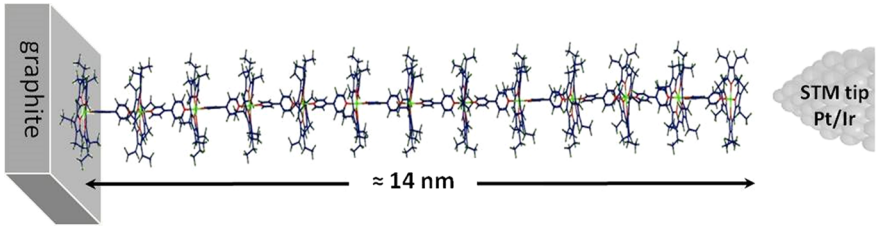

Figure 1. Scheme of a 14 nm long molecular wire, consisting on alternating ZnOEP and BP units, as obtained by SPARTAN software (Wavefunction, Inc.).

around 30 nm, which implies that tens or hundreds of molecules are contacted at the same time. In addition, it is not easy to control the force that the tip exerts over the molecules (organized as monolayers), and consequently, it is difficult to discard contributions arising from direct current between the tip and the substrate. The STM break junction technique is one of the most reliable to assess the electrical properties at the single molecule level.[18] There is no gap between the tip and the molecule, being the STM tip really connected (bonded) to the molecule. However, binding a molecule to electrodes affects its structure and consequently vibrational characteristics, as evidenced by inelastic tunneling spectroscopy,[19] which, in turn, influence the charge transport.

An additional difficulty when studying molecular systems prepared by self-assembly from solutions relates to the possible existence of polymorphism, metastable phases extending up to hours.[20−22] Any molecular movements taking place while recording the I/V characteristics are expected to affect the measured current. In fact, it was observed that molecular packing and order affect the electrical transport across self-assembled monolayers.[23] It follows that rationalization of electrical properties of assembled monolayers at the single molecule level requires a good knowledge of molecular ordering/orientation on the surface. Combined topographic and electrical (current) studies on organic monolayers have been carried out, both under ambient conditions (air) and at the solid/liquid interface, using the spectroscopy tool of STM, which is often referred to as scanning tunneling spectroscopy (STS).[24] Usually the tip is stopped over the molecule and the current is measured as a function of the bias applied between the tip and the sample. The main disadvantage of this technique is the existence of a gap between the tip and the molecule, which leads to an additional resistance. However, as the high resolution of this technique allows the measurement of current at the single molecule level with high precision and stability, it remains very powerful and widely used. For instance, STS has been used to analyze self-assembled monolayers at the graphite−liquid interface.[25] A recent review, by Lei and De Feyter,[25] provides a very comprehensive report on the use of STS to study various self-assembled monolayers, both under ambient conditions and at the solid−liquid interface.

The electrical properties of molecular wires at the single molecule level have been mostly limited to molecules or supramolecular structures that are just a few nanometers (3−4 nm) long. Among the few exceptions, Ashwell et al.[26] reported single-molecule electronic properties of self-assembled arylene-ethylene molecular wires with 7 nm in length using the Haiss method.[27] The current is monitored as a function of time aiming to detect a chemical contact between the tip and molecule. Once such contact is achieved, the current is recorded allowing the determination of the wire conductance. Other studies, on long molecular wires, rely on the use of techniques that assess a large number of wires, such as conducting AFM[3,4] or the mercury drop technique.[28] No doubt this is an area where a long debate is still taking place, not only related to the different methods being used but also with the nature of the transport across molecular wires and the influence of their structure.

Here, we report on the electrical behavior of molecular wires with lengths up to 14 nm, fabricated in a step-by-step process, consisting on zinc(II)octaethylporphyrin (ZnOEP) alternating with 4,4′-bipyridine (BP), a conductive bridge. We have recently reported on this controlled method to fabricate well-defined molecular wires, with a real time monitoring of the wires growth process using STM.[29] Figure 1 shows the molecular model of the longest molecular wire we prepared, made of 25 individual molecules, which are arranged in a well-defined sequence and assembled in a stepwise fashion, via bonding (complexation) between the central metal of the porphyrin unit (Zn) and the nitrogen atom of bypiridine. This resembles a living coordination polymerization, which ensures an epitaxial-like growth of the wires. In fact, the binding energy between pyridine and ZnOEP was calculated by DFT as being 56.9 kJ/mol, a value that is in good agreement with the reported binding energy of NH_3 to zinc(II)-tetraphenylporphyrin (49 kJ/mol).[30] The sequential addition of these building blocks results in the formation of monolayers, a process that was monitored by STM imaging along each growth step, to evidence that the entire surface is made of a packed, well-defined monolayer. This monitoring is critical because ZnOEP was shown to exhibit a polymorphic behavior on highly oriented pyrolitic graphite (HOPG), with the ZnOEP monolayer taking ca. 3 h to achieve the most stable structure.[20] We therefore want to ensure that, at every step of ZnOEP addition, a well-organized and packed monolayer is formed, before proceeding to the next monolayer. In addition to this imaging, we have also performed, at each step of the wire growth, STS measurements, to assess the electrical properties of the formed wires. Thereby, hundreds of I/V curves were recorded at each wire growth step (i.e., at each monolayer).

2. EXPERIMENTAL SECTION

2.1. Molecular Wires Preparation. The molecular wires were prepared using a previously described stepwise procedure.[30] Porphyrin molecules were adsorbed on HOPG (MikroMasch) from a saturated solution of ZnOEP (Aldrich) in tetradecane (Aldrich). A drop of this solution was added between the STM tip and the HOPG substrate, and STM images were recorded from that moment on. The adsorption process is thus monitored until a full coverage of the substrate by a stable organization of the porphyrin molecules is achieved. This functionalized substrate is then immersed in a dilute

dx.doi.org/10.1021/jp501122n | J. Phys. Chem. C 2014, 118, 7229−7234

solution of 4,4′-bipyridine (Aldrich) in tetradecane for 1 min. It is afterward washed with tetradecane and imaged by STM before proceeding to the next ZnOEP monolayer formation.

2.2. STM/STS Measurements. STM images were obtained using a Molecular Imaging microscope, model 5100 from Agilent Technologies, with a mechanically cut Pt/Ir (70/30) metallic wire with a diameter of 0.25 mm (Goodfellow) as tip. All measurements were performed at room temperature at the HOPG/tetradecane interface. STS consisted on the measurement of I/V curves during the image (topography) scanning at predefined positions. The tip stops at each marker, the feedback loop is temporally disabled, and a voltage sweep between −1.0 and +1.0 V is applied between the tip and substrate. More than 400 curves were collected for each monolayer from 5 different samples where a different STM tip was used to each one. Their statistical analysis was carried out using algorithms running in Matlab.

3. RESULTS AND DISCUSSION

3.1. Porphyrin Self-Assembled Monolayer on HOPG. The first step of the molecular wires growth is the functionalization of the HOPG surface with ZnOEP. A ZnOEP monolayer was self-assembled on the graphite surface, being its structure monitored by STM at the HOPG/tetradecane interface. Once a fully packed monolayer was formed, with an hexagonal arrangement (most stable packing),[20,29] fully covering the HOPG surface, it was characterized by STS. Figure 2 shows a STM image of a ZnOEP monolayer with 7 markers, A to G, corresponding to the positions of porphyrin molecules where the I/V curves were recorded. The inset of Figure 2 shows the recorded data. A total of 2500 I/V curves were collected on this ZnOEP monolayer, and the conductance was calculated from the slope of these curves in the ohmic region (between −0.2 and +0.2 V). A statistical analysis was made on this data, using the procedure reported by Zhang et al.[31] for the STS study of single molecules on Au(111). In such study, Zhang et al. collected all conductance values in a histogram and attributed the obtained distribution of conductance values to a distribution of the number of molecules interacting simultaneously with the STM tip. Similarly, a histogram was made here, collecting all conductance values we obtained, and the distribution was fitted by three Gaussian functions, as shown in Figure 3. The average conductance values of each of these Gaussian functions (that is the conductance corresponding to the maximum of each function) are $0.14 \times 10^{-5}G_0$, $0.26 \times 10^{-5}G_0$, and $0.51 \times 10^{-5}G_0$. The histogram shows a more pronounced first peak, followed by satellite peaks, whose positions are close to multiples of the first one: $I_n \approx nI_1$. We assume, as in refs 31 and 32, that these three peaks correspond to 1, 2, and 3 single wires, respectively, interacting simultaneously with the STM tip. Though this assignment is not unambiguous, we are confident that the peak with lower conductance approaches the conductance of a single wire.

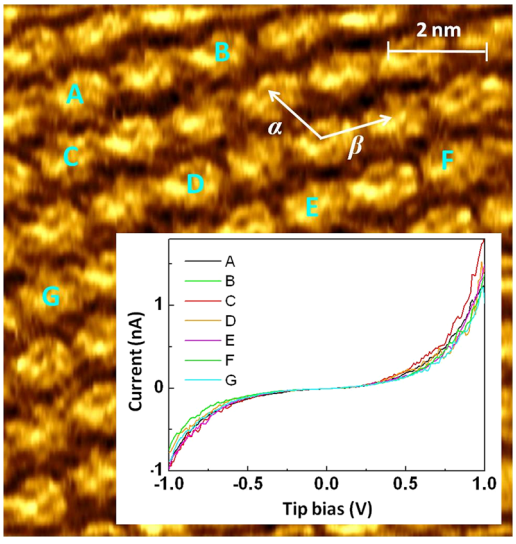

Figure 2. High-resolution STM image (10×10 nm^2) of a ZnOEP monolayer on HOPG obtained by the tetradecane/HOPG interface technique (tunneling conditions: I_t = 224 pA, U_t = 560 mV) and with unit cell parameters: $\alpha = 1.40 \pm 0.05$ nm, $\beta = 1.38 \pm 0{:}08$ nm, and the angle between the two is $\gamma = 115 \pm 1°$. The letters identify the locations where I/V curves were collected by sweeping the voltage from −1.0 to +1.0 V during 10 s. The inset shows the corresponding plot.

3.2. Molecular Wires. Following HOPG surface functionalization, the molecular wires were fabricated upon alternating binding of 4,4′-bipyridine and ZnOEP. In this study, the longest molecular wire contains a total of 13 porphyrins separated by 12 bipyridine units. The final supramolecular structure is a vertical molecular wire, 14.29 nm in length. The total length was determined by density functional theory (B3LYP method with 6-31G* basis set) using a SPARTAN software (Wavefunction, Inc.). In this calculation, we considered that the ethyl groups of the first porphyrin (the one that functionalizes the HOPG surface) are turned to the graphite and that the ethyl groups of the last one are turned upward. The electrical measurements were made at every growth step of the wires. STS studies were only carried out when, based on the STM imaging, a fully packed and defect free monolayer was formed. I/V curves were recorded only when the STM tip was on top of a molecule site. Figure 4a shows the incomplete fourth monolayer made of BP (identified as BP4) assembled on the second ZnOEP unit (3rd building block of the wire, identified as ZnOEP3), with a clearly visible defect and evidencing the presence of porphyrins from the previous monolayer. Figure 4b shows a high-resolution image of the ninth monolayer composed by porphyrins and where a defect shows the underlying monolayer of bipyridine. Quite surprisingly, the STM image resolution was maintained during the entire molecular wire building process until the last monolayer we assembled to finish the wire. Figures S1.1 to S1.22 of the Supporting Information show STM images of monolayers 1 up to 22. The monolayer 23 still maintains the high resolution, as shown in the Figure 4c, where each brighter point represents a porphyrin. The hexagonal porphyrin arrangement shown in Figure 4c and its unit cell dimensions ($(\alpha = 1.4 \pm 0.1)$ nm, $\beta = (1.3 \pm 0.1)$ nm, and the angle between the two is $\gamma = (110 \pm 5)°$) are similar to those of the first monolayer (as is indicated in Figure 2). Hundreds of I/V curves were collected for all monolayers, and they were combined in histograms, as described above (Figure 3). All histograms are shown in Table S2.1 of the Supporting Information. They were fitted with Gaussian curves from which we obtained the average/peaks conductance. The values are listed in Table S2.1 of the Supporting Information. Using the procedure described above, we considered the conductance corresponding to the first peak as the wire conductance. Figure

dx.doi.org/10.1021/jp501122n | J. Phys. Chem. C 2014, 118, 7229−7234

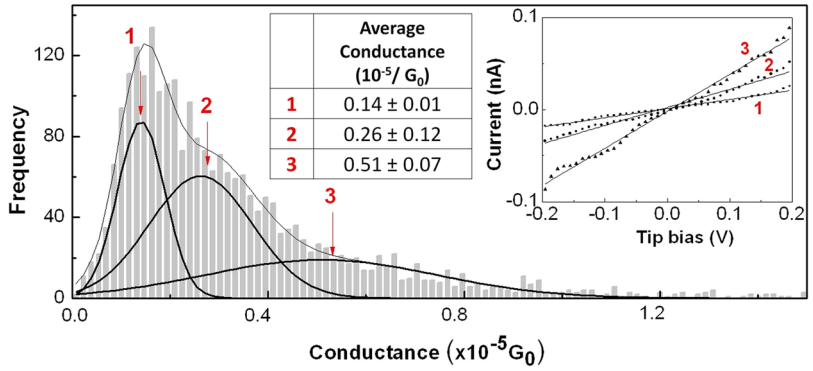

Figure 3. Conductance histogram constructed from over 2500 individual current−voltage curves. The right-hand side inset shows the I/V curves, in the ohmic region, corresponding to the three peaks of the conductance distribution (solid lines are linear fits). Inset at the center: average value of the Gaussian distribution.

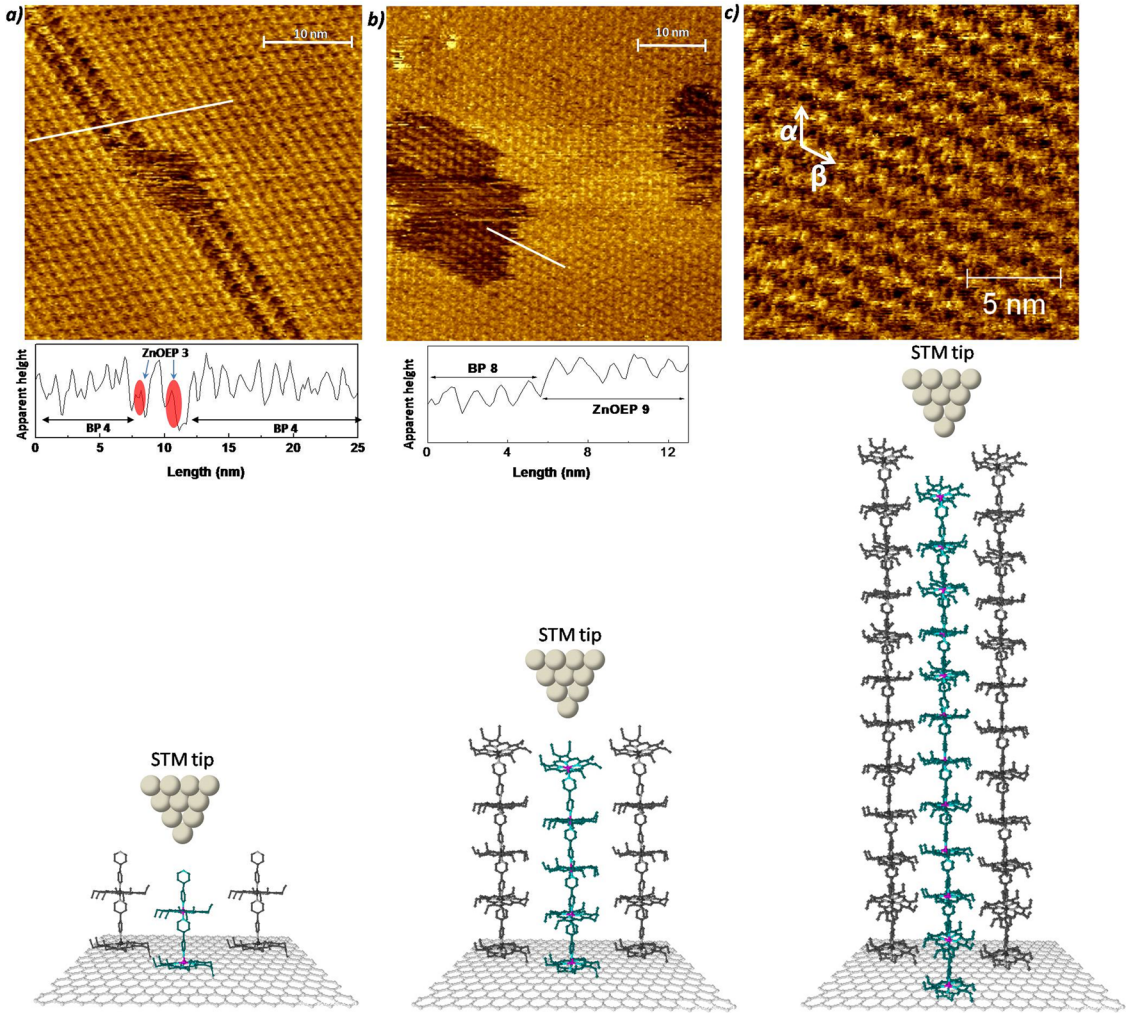

Figure 4. (a)STM image (0.117 nA and 0.7 V) of a fourth self-assembled monolayer composed by bipyridines. The darker stripes are regions without BP molecules and where it is possible to observe the underlying porphyrin monolayer. The bottom graph shows a line profile of the white line marked on the image. The bottom scheme shows molecular wires composed by two porphyrins linked by bypiridines. (b) STM image (0.115 nA and 1.3 V) of the ninth monolayer composed by ZnOEP molecules where the darker regions are due to bipyridine molecules of the eighth monolayer. The bottom graph is a line profile that evidences the height difference between the two monolayers. The bottom scheme shows molecular wires composed by five porphyrins linked by bypiridines. (c) High-resolution STM image (0.174 nA and 1.39 V) of the 23rd (last) monolayer composed by porphyrin molecules where the white vectors define the unit cell (α = (1.4 ± 0.1) nm, β = (1.3 ± 0.1) nm, and the angle between the two is γ = (110 ± 5)°). The scheme shows molecular wires composed by 12 porphyrins linked by bypiridines.

5 shows a plot of the molecular wires resistance as a function of their length, where a change in behavior is observed at ca. 6.5 nm. This transition reflects the change in the prevalent conduction mechanism,[3,4] with the tunneling mechanism

dx.doi.org/10.1021/jp501122n | J. Phys. Chem. C 2014, 118, 7229−7234

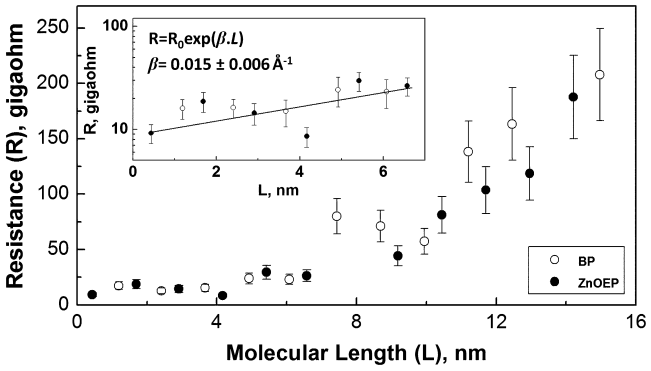

Figure 5. Resistance (R) as a function of molecular wire length (L). Each experimental point was determined by the minimum conductance values represented in the conductance histograms constructed from over thousands of current−voltage curves obtained from each monolayer (see Supporting Information). The inset shows a semilog plot of R versus L for wires with lengths up to ca. 6.5 nm and the fit to eq 1. The resistance represented in the graphic is the contribution of the molecular resistance and the resistance from the gap between the tip and the molecule.

being dominant for shorter molecular wires, while for longer wires a hopping mechanism prevails.

For shorter wires, the resistance has an exponential dependence on the length, as shown in the inset of Figure 5. The length dependence of the electrical resistance was fitted with eq 1, up to a length of 6.5 nm. From that fit, a very low attenuation factor ($\beta = 0.015 \pm 0.006$ Å^{-1}) is obtained and is in agreement with the oligoporphyrin molecular wires reported by Nichols et al.[5,6] They reported ultralow β values for different types of porphyrin based molecular wires and concluded that these have the lowest attenuation factor yet reported for single-molecule conductance by a series of organic molecules. The authors also concluded that the wires composed by porphyrins linked by axial coordination chemistry improves the electronic transport where the lowest β factor was found for β-fused taped oligoporphyrins ($\beta = 0.02$ Å^{-1}).[6] Our attenuation factor is even lower suggesting that the electric transport can be improved if the porphyins are linked by the metal center instead of the axial coordination presented by Nichols et al.

For wires longer than 6.5 nm, the resistance is considerably greater and increase linearly with the length, which is indicative of the presence of hopping regime. The transition to hopping regimes for wires longer than 6.5 nm is not unusual and was previously observed using conductive AFM where a threshold length of 4−5 nm was determined.[4,33] The STS method used to measure the molecular conductance could have some influence since the tunneling distance between the STM tip and the top of wires (below 1 nm) could affect the region of the electronic regime transition. However, additional studies regarding the electrical transport in longer molecular wires are needed in order to reveal these mechanisms, and the porphyrin based molecular wires are interesting candidates to do this.

4. CONCLUSIONS

To conclude, the STS analysis of molecular wires composed by alternating porphyrins and bipyridines shows that these materials can have important applications in molecular electronics. The system is able to transport charge until 14 nm and has a weak dependence on the length. Furthermore, the high-resolution STM images proves that it is a stable system in terms of molecular order and packing, and this is the main reason for the efficiency of the electrical transport. This system could be a starting point to explore similar supramolecular systems in order to improve its electrical characteristics.

■ ASSOCIATED CONTENT

Supporting Information

STM images of all units that compose the molecular wires and monolayers (porphyrins and bypiridines), histograms of individual I/V curves. This material is available free of charge via the Internet at http://pubs.acs.org.

■ AUTHOR INFORMATION

Corresponding Author

*(Q.F.) E-mail: quirina.ferreira@lx.it.pt.

Author Contributions

The manuscript was written through contributions of all authors. All authors have given approval to the final version of the manuscript.

Notes

The authors declare no competing financial interest.

■ ACKNOWLEDGMENTS

The authors thank FCT-Portugal for financial support under the projects PEst-OE/EEI/LA0008/2013 and EXPL/CTM-NAN/0837/2012 and Post-Doc grant to QF.

■ REFERENCES

(1) Metzger, R. Unimolecular Electronics. *J. Mater. Chem.* **2008**, *18*, 4364−4396.

(2) Choi, S. H.; Frisbie, C. D. *Charge and Exciton Transport Through Molecular Wires*; Wiley-VCH Verlag GmbH &KGaA: Weinheim, Germany, 2011.

(3) Choi, S. H.; Frisbie, C. D. Enhanced Hopping Conductivity in Low Band Gap Donor−Acceptor Molecular Wires Up to 20 nm in Length. *J. Am. Chem. Soc.* **2010**, *132*, 16191−16201.

(4) Choi, S. H.; Kim, B. S.; Frisbie, C. D. Electrical Resistance of Long Conjugated Molecular Wires. *Science* **2008**, *320*, 1482−1486.

(5) Sedghi, G.; Garca-Surez, V.; Esdaile, L.; Anderson, H.; Lambert, C.; Martn, S.; Bethell, D.; Higgins, S.; Elliot, M.; Bennett, N.; et al. Long-Range Electron Tunnelling in Oligo-Porphyrin Molecular Wires. *Nat. Nanotechnol.* **2011**, *6*, 517.

(6) Sedghi, G.; Esdaile, L.; Anderson, H.; Martin, S.; Bethell, D.; Higgins, S.; Nichols, R. Comparison of the Conductance of Three Types of Porphyrin-Based Molecular Wires: *β,meso, β*-Fused Tapes, *meso*-Butadiyne-Linked and Twisted *meso-meso* Linked Oligomers. *Adv. Mater.* **2012**, *24*, 653−657.

(7) Yoon, D.; Lee, S.; Yoo, K.; Kim, J.; Lim, J.; Aratani, N.; Tsuda, A.; Osuka, A.; Kim, D. Electrical Conduction through Linear Porphyrin Arrays. *J. Am. Chem. Soc.* **2003**, *125*, 11062−11064.

(8) Susumu, K.; Frail, P.; Angiolillo, P.; Therien, M. Conjugated Chromophore Arrays with Unusually Large Hole Polaron Delocalization Lengths. *J. Am. Chem. Soc.* **2006**, *128*, 8380−8381.

(9) Sedghi, G.; Sawada, K.; Esdaile, L.; Hoffmann, M.; Anderson, H.; Bethell, D.; Haiss, W.; Higgins, S.; Nichols, R. Single Molecule Conductance of Porphyrin Wires with Ultralow Attenuation. *J. Am. Chem. Soc.* **2008**, *130*, 8582−8583.

(10) Salomon, A.; Cahen, D.; Lindsay, S.; Tomfohr, J.; Engelkes, V.; Frisbie, C. Comparison of Electronic Transport Measurements on Organic Molecules. *Adv. Mater.* **2003**, *15*, 1881−1890.

(11) Chen, F.; Li, X.; Hihath, J.; Huang, Z.; Tao, N. Effect of Anchoring Groups on Single-Molecule Conductance: Comparative Study of Thiol-, Amine-, and Carboxylic-Acid-Terminated Molecules. *J. Am. Chem. Soc.* **2006**, *128*, 15874−15881.

(12) Heath, J.; Ratner, M. Molecular Electronics. *Phys. Today* **2003**, *56*, 43−49.
(13) Tao, N. J. Electron Transport in Molecular Junctions. *Nat. Nanotechnol.* **2006**, *1*, 173−181.
(14) Fatemi, V.; Kamenetska, M.; Neaton, J.; Venkataraman, L. Environmental Control of Single-Molecule Junction Transport. *Nano Lett.* **2011**, *11*, 1988−1992.
(15) Liu, H.; Wang, N.; Zhao, J.; Guo, Y.; Yin, X.; Boey, F.; Zhang, H. Length-Dependent Conductance of Molecular Wires and Contact Resistance in Metal−Molecule−Metal Junctions. *ChemPhysChem* **2008**, *9*, 1416−1424.
(16) Wolf, D.; Haag, R.; Rampi, M.; Frisbie, C. Distance Dependence of Electron Tunneling through Self-Assembled Monolayers Measured by Conducting Probe Atomic Force Microscopy: Unsaturated versus Saturated Molecular Junctions. *J. Phys. Chem. B* **2002**, *106*, 2813−2816.
(17) Xu, B.; Tao, N. Measurement of Single-Molecule Resistance by Repeated Formation of Molecular Junctions. *Science* **2003**, *301*, 1221−1223.
(18) Xu, B.; Xiao, X.; Tao, N. Measurements of Single-Molecule Electromechanical Properties. *J. Am. Chem. Soc.* **2003**, *125*, 16164−16165.
(19) Stipe, B.; Rezaei, M.; Ho, W. Single-Molecule Vibrational Spectroscopy and Microscopy. *Science* **1998**, *280*, 1732−1735.
(20) Ferreira, Q.; Bragança, A.; Moura, N.; Faustino, M.; Alcácer, L.; Morgado, J. Dynamics of Porphyrin Adsorption on Highly Oriented Pyrolytic Graphite Monitored by Scanning Tunnelling Microscopy at the Liquid/Solid Interface. *Appl. Surf. Sci.* **2013**, *273*, 220−225.
(21) Bonini, M.; Zalewski, L.; Breiner, T.; Ötz, F.; Kastler, M.; Schälder, V.; Surin, M.; Lazzaroni, R.; Samori, P. Competitive Physisorption Among Alkyl-Substituted π-Conjugated Oligomers at the Solid−Liquid Interface: Towards Prediction of Self-Assembly at Surfaces from a Multicomponent Solution. *Small* **2009**, *5*, 1521−1526.
(22) Piot, L.; Marchenko, A.; Wu, J.; Müllen, K.; Fichou, D. Structural Evolution of Hexa-*peri*-hexabenzocoronene Adlayers in Heteroepitaxy on *n*-Pentacontane Template Monolayers. *J. Am. Chem. Soc.* **2005**, *127*, 16245−16250.
(23) Dholakia, G.; Fan, W.; Meyyappan, M. Effect of Monolayer Order and Dynamics on the Electronic Transport of Molecular Wires. *Appl. Phys. A: Mater. Sci. Process.* **2005**, *80*, 1215−1223.
(24) Hipps, K. *Handbook of Applied Solid State Spectroscopy*; Springer: New York, 2006.
(25) Lei, S.; Feyter, S. *STM and AFM Studies on (Bio)molecular Systems:Unravelling the Nanoworld*; Springer: Berlin, Germany, 2008.
(26) Ashwell, G. J.; Urasinska, B.; Wang, C.; Bryce, M. R.; Gracec, I.; Lambert, C. J. Single-Molecule Electrical Studies on a 7 nm Long Molecular Wire. *Chem. Commun.* **2006**, *45*, 4706−4708.
(27) Nichols, R.; Haiss, W.; Higgins, S.; Leary, E.; Martin, S.; Bethell, D. The Experimental Determination of the Conductance of Single Molecules. *Phys. Chem. Chem. Phys.* **2010**, *12*, 2801−2815.
(28) Tuccitto, N.; Ferri, V.; Cavazzini, M.; Quici, S.; Zhavnerko, G.; Licciardello, A.; Rampi, M. Highly Conductive ∼40-nm-long Molecular Wires Assembled by Stepwise Incorporation of Metal Centres. *Nat. Mater.* **2009**, *8*, 41−46.
(29) Ferreira, Q.; Alcácer, L.; Morgado, J. Stepwise Preparation and Characterization of Molecular Wires Made of Zinc Octaethylporphyrin Complexes Bridged by 4,4′-bipyridine on HOPG. *Nanotechnology* **2011**, *22*, 435604.
(30) Hieringer, W.; Flechtner, K.; Kretschmann, A.; Seufert, K.; Auwrter, W.; Barth, J.; Garling, A.; Steinrck, H.; Gottfried, J. The Surface Trans Effect: Influence of Axial Ligands on the Surface Chemical Bonds of Adsorbed Metalloporphyrins. *J. Am. Chem. Soc.* **2011**, *133*, 6206−6222.
(31) Zhang, Y.; Dou, C.; Wang, Y. Single-Molecule Conductance Measurement of Self-Assembled Organic Monolayers Using Scanning Tunneling Spectroscopy in Combination with Statistics Analysis. *Appl. Surf. Sci.* **2011**, *257*, 6514−6517.
(32) Li, C.; Pobelov, I.; Wandlowski, T.; Bagrets, A.; Arnold, A.; Evers, F. Charge Transport in Single Au 'Alkanedithiol' Au Junctions: Coordination Geometries and Conformational Degrees of Freedom. *J. Am. Chem. Soc* . **2008**, *130*, 318−326.
(33) Luo, L.; Frisbie, C. Length-Dependent Conductance of Conjugated Molecular Wires Synthesized by Stepwise "Click" Chemistry. *J. Am. Chem. Soc.* **2010**, *132*, 8854−8855.